Journal of Solid State Chemistry **157,** 220–224 (2001)
doi:10.1006/jssc.2000.9079, available online at http://www.idealibrary.com on IDEAL®

Correlation and Relativistic Effects in β-PbO and Other Lead (II) Oxides: A Quantum *ab Initio* Explanation of ^{207}Pb NMR and XANES Spectra

C. Dybowski,* S. P. Gabuda,†,‡ S. G. Kozlova,†,‡ G. Neue,§ D. L. Perry,¶ and V. V. Terskikh‡

*Department of Chemistry and Biochemistry, University of Delaware, Newark, Delaware 19716; †Inorganic Chemistry Institute, 630090 Novosibirsk, Russia; ‡Steacie Institute for Molecular Sciences, National Research Council of Canada, Ottawa K1A OR6, Canada; §Department of Physical Chemistry, University of Dortmund, D-44221, Dortmund, Germany; and ¶Lawrence Berkeley National Laboratory, University of California—Berkeley, California 94720

Received September 19, 2000; in revised form December 4, 2000; accepted December 8, 2000

We examine correlation and relativistic effects on Pb–Pb and Pb–O interactions in β-PbO with *ab initio* quantum calculations and ^{207}Pb NMR chemical-shift-tensor analysis. We find a covalent-like Pb^{2+}–Pb^{2+} interaction accounts for many facets of the NMR spectroscopy and the X-ray absorption near-edge structure, as well as other spectroscopic properties. This covalent effect arises from the relativistic properties of the $6p_{3/2(m=\pm 1/2)}$ and $6p_{3/2(m=\pm 1/2)}$ orbitals. The existence of such interactions in lead (II) oxides other than β-PbO may explain NMR and optical spectra of these materials as well.

Key Words: **lead oxides; solid-state NMR; quantum *ab initio* calculations; relativistic effects.**

INTRODUCTION

Spectroscopic and structural measurements of solid lead oxides present several interesting and unusual features of these materials. NMR lines are more shielded than Pb^{2+} ions surrounded by oxygen-containing species in other materials (1). Lead (II) monoxide is known to crystallize not in the simple cubic NaCl structure, as might be expected, but in two forms of lower symmetry, α-PbO and β-PbO. The lower symmetry of these materials is exhibited as single layers of oxygen in α-PbO and twinned layers in β-PbO, between which are sandwiched layers of lead (2–5). The four closest interlayer Pb … Pb contacts are at 383 pm in α-PbO; there are two similar contacts in β-PbO at 397.7 pm and two at 420 pm (Fig. 1). Such distances are sufficiently long that one usually associates them with a lack of strong bonding interactions. Nevertheless, both α-PbO and β-PbO exhibit neither perfect clevage nor anisotropy of thermal expansion coefficients (5). Yet another indicator of unusual interactions in these materials is the fact that, contrary to expectation based on the interlead distances, β-PbO is more stable than α-PbO. For example, the experimental interlayer Pb ⋯ Pb force constant of β-PbO (f(Pb–Pb) = 0.65 N/cm) is nearly twice that of α-PbO (f(Pb–Pb) = 0.3 N/cm) (6, 7), indicating substantially different intermolecular Pb … Pb interactions in the two modifications. However, extended Hückel tight-binding calculations (8) do not elucidate the difference in bonding between Pb atoms. In density-functional theories (DFT) (9, 10) the possible Pb … Pb interactions in the lead oxides are related to hybridization between the Pb 6*s* and the O 2*p* orbitals, which would lead to the formation of Pb "lone pairs," but the difference in Pb … Pb interactions in two PbO polymorphs remains to be investigated.

Here we propose a model of 6*s*–6*p* promotion in the Pb^{2+} ions of the two monoxides that produces a covalent-like Pb … Pb interaction (1) that, in principle, qualtitatively explains the differences in the NMR spectroscopy. The model is supported by X-ray absorption near-edge structure (XANES) of these materials, showing that the electronic structure depends critically on structural form (11). The proposed interactions are important features of these materials, so we explore them theoretically in this paper. The results of ab initio calculations demonstrate that a structural stabilization occurs, amounting to a covalent-like interaction between two Pb centers when relativistic effects are included.

^{207}Pb NMR Magnetic-Shielding Tensor of β-PbO

The inference of Pb–O and Pb–Pb interactions in β-PbO derives from analysis of the ^{207}Pb magnetic-shielding tensor σ, similar to that of minium (12). Its principal components, $\{\sigma_{ii}\}$, are determined by structural and bonding parameters of the Pb^{2+} local site through the simple form (13)

$$\sigma_{ii} = -\Sigma_k A_k \sin^2 \Theta_{ik}. \qquad [1]$$

0022-4596/01 $35.00

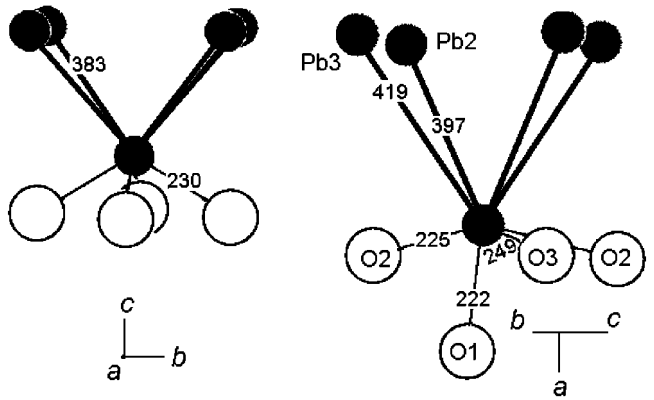

FIG. 1. The coordination of Pb in α-PbO (left) and β-PbO (right). All distances are in picometers.

Θ_{ik} is the angle between the ith principal axis of the tensor and the Pb–Y_k vector. Y_k is a neighboring atom. The A_k's, regarded as experimentally determined parameters, are coefficients that collect the effects of electron density at various atoms on the lead chemical shielding. Theoretically, they are related to partial unquenching of angular momentum of Pb orbitals due to overlap with nearest-neighbor orbitals (14), and also to spin–orbit interaction (14, 15). In this model, possible π bonding is neglected.

Generally, one finds in the literature the NMR chemical-shift tensor, δ, relative to a standard material, in this case tetramethyllead (TML), rather than the magnetic shielding σ. The principal elements of the ^{207}Pb magnetic-shielding tensor, σ, are related to the principal elements of the chemical-shift tensor, δ, by the relation

$$\sigma_{ii} = \sigma(R) - \delta_{ii}, \qquad [2]$$

where $\sigma(R)$ is the absolute (isotropic) ^{207}Pb magnetic shielding of TML, and δ_{ii} are the principal elements of the ^{207}Pb NMR chemical-shift tensor. Uncertainty in the shielding arises from the lack of a direct method to measure absolute nuclear magnetic shielding for ^{207}Pb in some environments. Previously, we demonstrated an indirect estimation of this value for TML: $\sigma\ (R) = -7030 \pm 400$ ppm, calculated from differences of anisotropic components of the tensor (1).

Various reports (1, 16, 17) of the experimental chemical-shift principal elements δ_{11}, δ_{22}, δ_{33} determined at room temperature are collected in Table 1. The slight dispersion of values probably reflects a variation in experimental conditions under which they were determined (1, 16, 17). For purposes of discussion, and given that the difference of δ_{11} and δ_{22} is within the limits of the estimated error of σ (R), the tensor σ may be regarded as approximately axial, with $\sigma_\perp \approx \sigma_{11} \approx \sigma_{22} = \sigma(R) - \frac{1}{2}(\delta_{11} + \delta_{22})$. The parallel component $\sigma_\parallel = \sigma(R) - \delta_{33}$ of this tensor is more shielded than the perpendicular component, $\sigma_\perp$.

TABLE 1
Principal Values of the ^{207}Pb NMR Chemical-Shift Tensor of β-PbO[a]

δ_{11}	δ_{22}	δ_{33}	δ_{iso}	Reference
2820	2760	−1000	1525 ± 10	(1)
2944.7	2572.6	−972.3	1515 ± 5	(16)[b]
2950	2700	−1040	1536 ± 35	(17)[c]

[a]All data are im ppm relative to TML.
[b]Derived from data on a mixed sample of α-PbO and β-PbO (in ~1:3 ratio).
[c]Determined by the "point-by-point" method.

To calculate the parameters A_i of ^{207}Pb in β-PbO, we use neutron diffraction data for the positions of atoms in the unit cell (3, 4). The space group of β-PbO is orthorhombic, *Pbma*; $Z = 4$, with refined (6) unit cell dimensions of $a_o = 589.31$ pm, $b_o = 549.04$ pm, and $c_o = 475.28$ pm. The lattice is built up of bc layers formed by parallel alignment of infinite planar zigzag chains …–Pb–O–Pb–O… with very short Pb–O bond lengths: $D_1(\text{Pb–O}_1) = 222.1$ pm and $D_2(\text{Pb–O}_2) = 224.9$ pm, and a O_1–Pb–O_2 angle of 90.16°. In the bc layers, the chains are held together by interchain Pb–O_3–Pb bridges with $D_3(\text{Pb–O}_3) = 249$ pm. Considering only the effects of the two closest and nearly perpendicular Pb–O_1 and Pb–O_2 bonds, the main values of the shielding tensor σ_{ii} are expressible in terms of the coefficients:

$$\sigma_{11} = \sigma_\parallel = -(A_{O1} + A_{O2})\sin^2\pi/2 \approx -2A_{O1,2} \qquad [3a]$$

$$\sigma_{22} = \sigma_{33} = \sigma_\perp = -(A_{O1} + A_{O2})\sin^2\pi/4 \approx -A_{O1,2}. \qquad [3b]$$

The orientations of the main axes of the magnetic-shielding tensor are expected to coincide with the O_1–Pb–O_2 triangle symmetry axes. We neglect the small difference between $A_{O1} = A(\text{Pb–O}_1)$ and $A_{O2} = A(\text{Pb–O}_2)$. Under these assumptions, the predicted perpendicular component $\sigma_\perp$ is more shielded than the longitudinal component, $\sigma_\parallel$, a result in disagreement with the experimental results. Thus, there must be other contributions than the effects of the neighboring oxygens. The inclusion of two more distant Pb–O_3 bonds does not qualitatively change the relation between $\sigma_\parallel$ and $\sigma_\perp$ because the Pb–O overlap (and A_O(Pb–O)) decreases exponentially with increasing Pb–O distance. Therefore, it may be concluded that including only the effects of nearest-neighbor interactions Pb–O_1, Pb–O_2, Pb–O_3 does not explain the observed symmetry of the magnetic-shielding tensor in β-PbO.

If not the oxygens, one must include nearest-neighbor Pb–Pb interactions. In β-PbO (3–5), with a distorted NaCl-like structure, each Pb is surrounded by 12 other lead centers at distances ranging from 353.6 to 475.28 pm. Among them are five Pb^{2+} ions disposed across the four closest anions O_1, O_2, $2O_3$. According to Gillespie's rule (18), these atoms may potentially participate in Pb–Pb bonding interactions, of which two involve intralayer couplings at a distances of $D(\text{Pb–Pb}_1) = 372.8$ pm, and four interlayer couplings, two at a distance of $D(\text{Pb–Pb}_2) = 397.7$ pm and another two at a distance of $D(\text{Pb–Pb}_3) = 419$ pm (Fig. 1). The central Pb atom and the atoms O_1, O_2, and Pb_3 lie in the symmetry plane *ab*; therefore one principal axis of the Pb magnetic-shielding tensor falls along the *c* axis, perpendicular to this plane. The value of this component, including the lead interactions, is determined by the coefficients in the manner

$$\sigma_{11} = -(A_{O1} + A_{O2} + A_{O3}\sin^2\Theta_{O3} + 2A_{Pb1}\sin^2\Theta_{Pb1} + 2A_{Pb2}\sin^2\Theta_{Pb2} + A_{Pb3}). \quad [4]$$

$A_{Pbi} = A(\text{Pb–Pb}_i)$, Θ_{Oi} and Θ_{Pbi} are the angles between the *c* axis and Pb–O_i and Pb–Pb_1 bonds, respectively (Table 2). The two other components, σ_{22} and σ_{33}, may be found from the angular dependence of the ^{207}Pb magnetic-shielding $\sigma_c(\varphi)$, where φ is the angle between the *b* axis and the orientation of the external magnetic field within the *ab* symmetry plane:

$$\sigma_c(\varphi) = -(\Sigma_i A_{Oi}\sin^2\Theta^c_{Oi} + \Sigma_i A_{Pbi}\sin^2\Theta^c_{Pbi}), \quad [5a]$$

$$\sigma_{22} = \min\sigma_c(\varphi);\ \sigma_{33} = \max\sigma_c(\varphi). \quad [5b]$$

$\Theta^c_i = \arccos[\cos(\pi/2 - \Theta_i)\cos(\varphi - \varphi^c_i)]$; φ^c_i is the angle between the *b* axis and the projection of the Pb–O_i or Pb–Pb_i vector on the *bc* plane (Table 2).

The simultaneous solution of Eqs. [4] and [5] is presented in the fourth line of Table 2. The symmetry axis (corresponding to σ_{33}) of the quasi-axial tensor makes an angle $\varphi^c_{33} = 74^\circ$ with the crystallographic *b* axis. Apart from the effects of Pb–O bonds, the largest contribution to the σ tensor is from two interlayer Pb–Pb_2 overlaps at a distance of 397.7 pm. Another contribution to σ is related to only the component along a single Pb–Pb_3 direction, which is nearly parallel to the O_1–Pb–O_2 bisector. This fact, along with the size of the Pb–Pb_3 distance, may be regarded as an indication of the spin–orbit nature of this contribution. The intralayer interaction between Pb and Pb_1 at 372.8 pm does not make a significant contribution, although the Pb–Pb_1 force constant (see Table 2) is nearly the same as that for Pb–Pb_3 (6, 7). This may indicate that the force constant $f(\text{Pb–Pb}_1)$ is not governed by the Pb–Pb_1 overlap. In other cases, there are strong observed correlations between the independent parameters A_i and f_i.

Pb^{2+} $6p_{3/2}$ Orbital Contribution to the Pb^{II} ... Pb^{II} Interaction

The fitting parameters A_i related to overlap of Pb orbitals with nearest-neighbor-atom (Y_i) orbitals may be calculated from characteristics of the Pb–Y_i bond through the equation (1, 13)

$$A_i = 8\,\mu_B{}^2\langle r^{-3}\rangle_p \Delta E^{-1}\Sigma_j S^2_{ij}, \quad [6]$$

where μ_B is the Bohr magneton, $\langle r^{-3}\rangle_p$ is the mean radial factor of the valence *p* orbital, ΔE is the mean single-electron excitation energy, S^2_{ij} are overlap integrals of Pb orbitals with the *j*th wave function of the nearest-neighbor atom, Y_i. The appreciable nonzero A_i values are direct indications that 6*p* orbitals participate in all intralyaer Pb–O_i bonds, as well as in interlayer Pb–Pb_2 bonds.

A further indicator of the importance of this interaction is found in XANES results for β-PbO (11). They show a dipole-allowed electronic transition from a filled 2*p* orbital to a Pb^{2+} 6*s* orbital, of almost the same intensity as a similar transition of PbO_2, where the Pb^{4+} 6*s* orbital is empty. However, for the usual divalent Pb^{II} state, such a transition should not be observed, because the 6*s* orbital is usually completely filled. For example, for $Pb(NO_3)_2$, there is no indication of a $2p \leftrightarrow 6s$ transition (11). This comparison clearly shows that, for β-PbO, 6*s*–6*p* promotion takes place.

In Table 3 the β-PbO NMR data are compared to those for α-PbO and Pb_3O_4 (1, 12). Interestingly, $A_i(\text{Pb–Pb}_i)$ values of β-PbO and Pb_3O_4 are almost twice that of α-PbO,

TABLE 2
Structural Parameters of Pb–Y_i Bonds in β-PbO

Pb–Y_i	Pb–O_1	Pb–O_2	Pb–O_3	Pb–Pb_1	Pb–Pb_2	Pb–Pb_3	Pb–Pb'_3
D_i(Pb–Y_i)(pm)	222.2	224.9	248.7	372.8	397.7	420.3	420.3
θ_i (°)	90	90	16.66	47.77	53.3	90	90
φ_i (°)	75.21	165.61	128.19	87.7	0	49.25	133.63
A_i(Pb–Y_i) (ppm)	2160	2460	650	0	2500	1940	0
f_i (N/cm)[a]	0.86	0.86	0.31	0.30	0.62	0.30	0

[a] Taken from references (7) and (8).

TABLE 3
Parameters for the Pb–O and Pb–Pb Bonds in Lead (II) Oxides

Lead (II) oxide	β-PbO	Pb_3O_4	α-PbO
D(Pb–O) (pm); (N)[a]	221; 222; 248 (2)	221.5 (2); 233.7	230 (4)
D(Pb–Pb) (pm)	397.4 (2); 419	380	383 (4)
A_O (ppm)	3200 (2); 1540 (2)	2960 (3)	1535 (4)
A_{Pb} (ppm)	3320	2880	1335 (4)

[a] Numbers in parentheses are coordination numbers.

although the Pb–Pb and Pb–O distances in these oxides are essentially the same (380–397 pm for Pb–Pb, and 222–230 pm for Pb–O). The only significant difference between β-PbO and Pb_3O_4, on the one hand, and α-PbO on the other is the nearest-neighbor coordination of Pb^{2+} by O^{2-}. For the first two compounds, it is two and four for α-PbO.

Extended Hückel calculations (19) demonstrate that 6*s*–6*p* mixing gives rise to an attractive interaction of the ions with the outer closed-shell configuration $6s^2$. In this case, the overlap population is positive (19), as must be for the case of a covalent interaction. Strong interactions of this kind may lead to vibronic instability of the high-symmetry configurations (20), even for systems with relatively large energy splittings (up to nearly 10 eV (20)) between the ground and excited states. As the excited $6p_{1/2}$ state of the Pb^{2+} ion is spherical, one would expect a vibronic instability of the NaCl-like configuration of PbO related to participation of an excited $6p_{3/2}$ ($m = \pm\frac{1}{2}$ and $m = \pm\frac{3}{2}$) orbital. An examination of the angular dependence of a relativistic $p_{3/2}$ orbital shows an elongated electron-density distribution for a $p_{3/2(m=\pm 1/2)}$ orbital (like a "dog-bone") and a flattened distribution for the $p_{3/2(m=\pm 3/2)}$ orbital (a "doughnut") (21). In square planar coordination (such as one would find for Pb^{2+} surrounded by four O^{2-} in α-PbO), the term nearest in energy to the $6s_{1/2}$ term is the $6p_{3/2(m=1/2)}$term. When Pb^{2+} is coordinated to two O^{2-} ions, as happens for β-PbO and Pb_3O_4, the term nearest in energy to the $6s_{1/2}$ will be the $6p_{3/2(m=3/2)}$. Thus, one would expect the Pb–Pb overlap in Eq. [4] to be appreciably different for α- and β-PbO because different $6p_{3/2}$ ($m = \pm\frac{1}{2}$ and $m = \pm\frac{3}{2}$) orbitals are involved in hybridization. This difference is the key to understanding the distinction in the molecular structure and bonding in different lead (II) oxides.

Contribution from Correlation Effects in the Pb … Pb Interaction

To demonstrate the covalent effect, we have calculated overlap integrals for a linear four-particle O–Pb … Pb–O cluster, using the program Jaguar 3.5 (22), with separated valence and core orbitals and the quasi-relativistic Hartree–Fock (HF) atomic wave functions of Cowan and Griffin (23) for Pb. Oxygen wave functions were represented by a 6-31G(p, d) atomic basis set. Generally, Pb–Pb interactions in such an approximation should be repulsive. We carried out two sets of calculations, first without inclusion of correlation effects, the second including correlation. To account for correlation effects that produce strong attraction between atoms or ions in closed-shell configurations (25), HF single-point calculations were carried out with the Jaguar 3.5 program package (22), including electron correlation corrections at the MP2 level (the second-order Möller–Plessed perturbation method (26)). To simplify calculations, we analyzed the Pb … Pb interaction potential $V[D(\text{Pb–Pb})]$ of a linear four-particle cluster O–Pb … Pb–O at different Pb–O distances: D(Pb–O) = 221, 231, and 237 pm, in both the HF and MP2 approximations. The results are shown in Fig. 2. The Hartree–Fock calculation does indeed show purely repulsive behavior, whereas in the MP2 approximation, there is a weakly attractive interaction between the leads. The minimum, however, is at a smaller Pb … Pb interatomic separation, D_e = 320–340 pm, than the experimental values, D(Pb–Pb) = 380 (Pb_3O_4), 384 (α-PbO), and 397 pm (β-PbO). The increase of the calculated interaction potential $V[D(\text{Pb–Pb})]$ with increasing Pb–O distance stands in contradiction to the experimental data (Table 3), because the actual Pb–Pb interaction drops sharply with small increases of the Pb–O distance in α-PbO relative to those of β-PbO and Pb_3O_4.

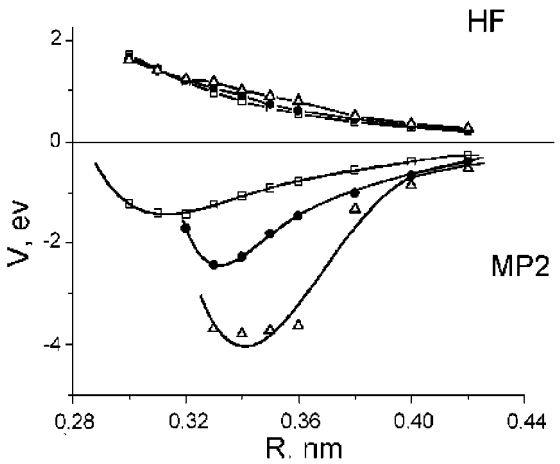

FIG. 2. The calculated dependence of the Pb … Pb intereaction potential, $\Delta E(R)$, on the lead–lead interatomic distance in a [O–Pb … Pb–O] cluster for various fixed values of the lead–oxygen distance. (□) D(Pb–O) = 221 pm; (●) D(Pb–O) = 231 pm; (Δ) D(Pb–O) = 237 pm. The purely repulsive behavior arises from Hartree–Fock (HF) calculations neglecting correlation, whereas the attractive curves result from the inclusion of correlation (MP2).

CONCLUSIONS

The analysis of the NMR spectroscopic data of β-PbO requires one to assume a significant covalent-like Pb^{2+}–Pb^{2+} interaction exists. Such an observation is consistent with the observed XANES spectroscopy of β-PbO, which shows strong 6*s*–6*p* promotion. The distorted, noncentrosymmetric O–Pb–O configurations in lead oxides create a strong intramolecular electric field (27) that acts on the Pb ion to trigger perturbative 6*s*–6*p* promotion. It is clear from the calculations that correlation effects create a bonding situation. However, the fact that inclusion of correlation does not predict the trends

in observed experimental results argues that strong Pb^{2+}–Pb^{2+} interactions in β-PbO, Pb_3O_4, and α-PbO probably do not originate exclusively in correlation effects, as found in other systems (25).

ACKNOWLEDGMENTS

S.P.G. and S.G.K. acknowledge the support of the Russian Fund for basic research Grant 99-03-32447. C.D. acknowledges the support of the Petroleum Research Fund of the American Chemical Society under Grant 33633-AC5. D.L.P. acknowledges the support of the U.S. Department of Energy under contract DE-AC-03-76SF00098. G.N. acknowledges the support of the Fonds der Chemischen Industrie.

REFERENCES

1. S. P. Gabuda, S. G. Kozlova, V. V. Terskikh, C. Dybowski, G. Neue, and D. L. Perry, *Chem. Phys. Lett*. **305,** 353–358 (1999).
2. J. Leciejewicz, *Acta Crystallogr*. **14,** 1304–1310 (1961).
3. J. Leciejewicz, *Acta Crystallogr*. **14,** 66–70 (1961).
4. M. I. Kay, *Acta Crystallogr*. **14,** 80–81 (1961).
5. R. J. Hill, *Acta Crystallogr. Sect. C* **41,** 1281–1284 (1985).
6. J. P. Vigouroux, E. Husson, G. Calvarin, and N. Dao, *Spectrochim. Acta A* **38,** 393–398 (1982).
7. J. P. Vigouroux, G. Calvarin, and E. Husson, *J. Solid State Chem.* **45,** 343–352 (1982).
8. G. Trinquer and R. Hoffman, *J. Phys. Chem.* **88,** 6696–6711 (1984).
9. H. Terpsta, R. A. deGroot, and C. Haas, *Phys. Rev. B* **52,** 11690–11696 (1995).
10. G. Watson, S. C. Parker, and G. Kresse, *Phys. Rev. B* **59,** 8481–8486 (1999).
11. S. Eiden-Assman, A.M. Schneider, P. Behrens, M. Wiebke, G. Engelhardt, and J. Felsche, *Chem. Eur. J*. **6,** 292–297 (2000).
12. S. P. Gabuda, S. G. Kozlova, V. V. Terskikh, C. Dybowski, G. Neue, and D. L. Perry, *Solid State NMR* **15,** 103–107 (1999).
13. N. F. Ramsey, *Phys. Rev*. **78,** 699–708 (1950).
14. C. P. Slichter, "Principles of Magnetic Resonance." Springer-Verlag, Heidelberg, 1980.
15. U. Edlund, T. Lejon, P. Pyykkö, T. K. Venkatachalam, and E. Buncel, *J. Am. Chem. Soc*. **109,** 5982–5985 (1987).
16. F. Fayon, I. Farnan, C. Bessada, J. D. Coutures, D. Massiot, and J. P. Coutures, *J. Am. Chem. Soc*. **119,** 6837–6843 **(**1997).
17. P. Zhao, S. Prasad, J. Huang, J. J. Fitzgerald, and J. S. Shore, *J. Phys.Chem. B* **103,** 10,617–10,626 (1999).
18. R. J. Gillespie, "Molecular Geometry." Van Nostrand-Reinhold, New York, 1972.
19. C. Janiak and R. Hoffmann, *J. Am. Chem. Soc*. **112,** 5924–5946 (1990).
20. I. B. Bersuker, "The Jahn–Teller Effect and Vibronic Interactions in Modern Chemistry," p. 320. Plenum, New York, 1984.
21. P. Pyykkö, *Chem. Rev*. **88,** 563–594 (1988).
22. Jaguar 3.5, Schroedinger, Inc., Portland, OR, 1998.
23. W. R. Wadt and P. J. Hay, *J. Chem. Phys*. **82,** 284–298 (1985).
24. P. C. Hariharan and J. A. Pople, *Theoret. Chim. Acta* **28,** 213–222 (1973).
25. P. Pyykkö, *Chem. Rev*. **97,** 597–636 (1997).
26. S. Saebö ad P. Pulay, *Theor. Chim. Acta* **69,** 357–368 (1986).
27. K. S. Pitzer, *J. Chem. Phys*. **63,** 1032–1033 (1975).